



DR ARIFUDDIN MOHAMMED (Orcid ID : 0000-0002-0158-5683)

DR INSAF AHMED QURESHI (Orcid ID : 0000-0001-7720-7067)

Article type : Research Article

Development of quinoline-based hybrid as inhibitor of methionine aminopeptidase 1 from *Leishmania donovani*

Short running title: Quinoline-based hybrid inhibits leishmanial MetAP1

Saleem Yousuf Bhat¹, Sonal Bhandari², Pavitra Suresh Thacker², Mohammed Arifuddin² and Insaf Ahmed Qureshi^{1*}

¹Department of Biotechnology & Bioinformatics, School of Life Sciences, University of Hyderabad, Prof. C.R. Rao Road, Hyderabad 500046, India

²Department of Medicinal Chemistry, National Institute of Pharmaceutical Education and Research (NIPER), Hyderabad 500037, India.

*E-mail: insaf@uohyd.ac.in

Abstract

Methionine aminopeptidase 1 (MetAP1) is a target for drug discovery against many adversaries and a potential antileishmanial target for its role in N-terminal methionine processing. As an effort towards new inhibitor discovery against methionine aminopeptidase 1 from *Leishmania donovani* (*LdMetAP1*), we have synthesized a series of quinoline-based hybrids i.e., (Z)-5-((Z)-benzylidene)-2-(quinolin-3-ylimino)thiazolidin-4-ones (QYT-4a-i) whose *in vitro* screening led to the discovery of a novel inhibitor molecule (QYT-4h) against *LdMetAP1*. The compound QYT-4h showed nearly 20-fold less potency for human MetAP1 and had drug-like features. Time-course

This article has been accepted for publication and undergone full peer review but has not been through the copyediting, typesetting, pagination and proofreading process, which may lead to differences between this version and the [Version of Record](#). Please cite this article as [doi: 10.1111/CBDD.13783](https://doi.org/10.1111/CBDD.13783)

This article is protected by copyright. All rights reserved

kinetic assays suggested QYT-4h acting through a competitive mode by binding to the metal activated catalytic site. Notably, QYT-4h was most potent against the physiologically relevant Mn(II) and Fe(II) activated forms of *LdMetAP1* and less potent against Co(II) activated form. Surface plasmon resonance and fluorescence spectroscopy demonstrated high affinity of QYT-4h for *LdMetAP1*. Through molecular modelling and docking studies, we found QYT-4h binding at the *LdMetAP1* catalytic pocket occupying both the catalytic and substrate binding sites mostly with hydrogen bonding and hydrophobic interactions which provides structural basis for its significant potency. These results demonstrate the feasibility of employing small molecule inhibitors for selective targeting of *LdMetAP1* which may find use to effectively eliminate leishmaniasis.

Keywords

Leishmania donovani; Methionine aminopeptidase 1; Quinoline-based hybrids; *In vitro* inhibition assay; Drug discovery.

1. Introduction

Leishmaniasis is one of the neglected tropical diseases representing a cluster of infections which are triggered by an intracellular parasitic protozoan appertaining to genus *Leishmania* (Burza, Croft, & Boelaert, 2018). This disease is fundamentally complex, featuring a string of clinical symptoms varying from cutaneous leishmaniasis (CL) with skin sores to mucocutaneous leishmaniasis (MCL) involving the mucous membrane to a deadly form called visceral leishmaniasis (VL). Over 20 *Leishmania* species have been found to propagate in highly affected regions with intriguing reports of spread in newer endemic areas (Thakur et al., 2018). Parasites *L. donovani* and *L. infantum/chagasi* complex trigger VL which is a systemic form of leishmaniasis. It is estimated that approximately 50,000 to 90,000 new cases of leishmaniasis occur every year, with most casualties emanating from VL (Alvar et al., 2012). Asymptomatic VL infections alongside infection sequela as post kala-azar dermal leishmaniasis (PKDL) build up the extra complexities of this ailment (Zijlstra, 2016). The commonly used medications encounter challenges of toxicity (Sundar & Chakravarty, 2010) and parasite resistance (Mohapatra, 2014), thus, highlighting the need to target parasitic pathways that are pivotal to the parasite's survival in the host and lethal to parasite when interrupted or inactivated.

Aminopeptidases excise amino acids by cleaving the peptide bond from the N-terminal end from oligopeptides or polypeptides (Bradshaw, 2013). Many families of aminopeptidases in particular

the M24 aminopeptidases play critical roles in parasite biology and N-terminal methionine processing, and have been increasingly targeted for drug development (Zhang et al., 2002; Chen et al., 2006). M24 aminopeptidases mainly comprise of methionine aminopeptidases which hydrolyze the initiator methionine residue from the N-terminus of newly synthesized polypeptides either co-translationally or post-translationally enabling critical post-translational modifications (Gigliione, Boularot, & Meinnel, 2004; Bhat, Dey, & Qureshi, 2018). This in turn ensures proper folding of proteins and enables protein function. For catalysis, the methionine aminopeptidases (MetAPs) require divalent metal co-factors in their catalytic site which is composed of two aspartates, two glutamates and a histidine residue (D'souza & Holz, 1999; Wang et al., 2003; Bhat, Dey, & Qureshi, 2018).

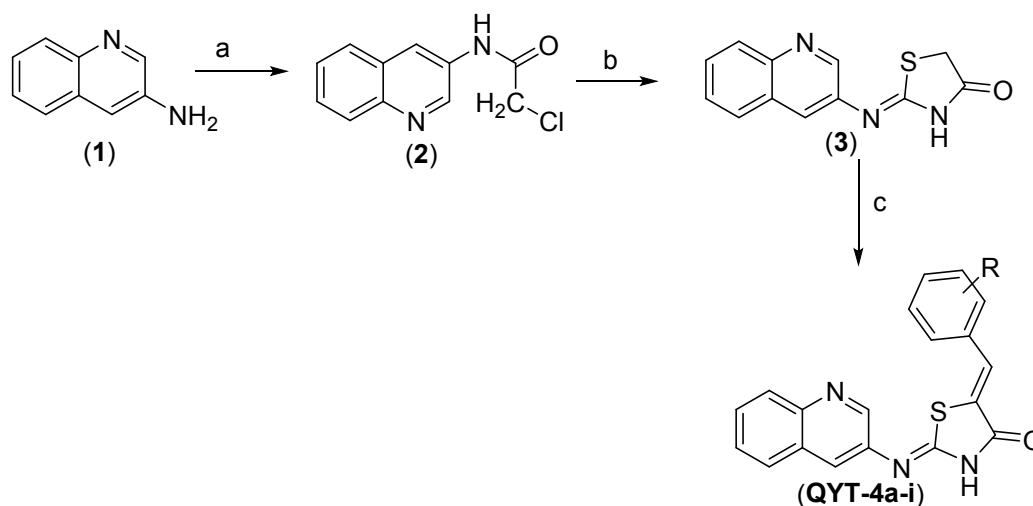
Eukaryotes including mammals and *Leishmania* species express two types of methionine aminopeptidases (Li & Chang, 2006; Frottin et al., 2016). One is a type I MetAP (MetAP1) and the other one being a type II MetAP (MetAP2) which carries an additional amino acid insertion towards the catalytic domain (Addlagatta, Hu, Liu, & Matthews, 2005). Eukaryotes develop lethal phenotypes if either one or both MetAP genes are deleted (Li & Chang, 2006). In contrast, prokaryotic genome encodes only type I MetAP which is reported to be essential (Chang, McGary, & Chang, 1989). Because MetAPs are essential enzymes, they have received attention as chemotherapeutic targets for the discovery of inhibitors or drug like chemical libraries against parasitic diseases such as malaria (Chen et al., 2006), neglected tropical diseases (Zhang et al., 2002), rheumatoid arthritis (Bernier et al., 2004) and grave adversaries like cancer (Yin, Wang, Zhang, & Liu, 2012).

We here report the synthesis and *in vitro* screening of quinoline-based hybrids [(Z)-5-((Z)-benzylidene)-2-(quinolin-3-ylimino)thiazolidin-4-ones] QYT-4a-i as selective inhibitors of *LdMetAP1*. With an array of biochemical and biophysical assays backed by computational approaches, we show the high affinity of QYT-4h [(2Z, 5Z)-5-((1H-indol-7-yl) methylene)-2-(quinolin-3-ylimino)thiazolidin-4-one] for *LdMetAP1* and dwell upon its selectivity and potential to guide the design and synthesis of highly selective and potent inhibitors against *LdMetAP1*.

2. Methodology

2.1 Synthesis of quinoline-based hybrids

The synthetic pathway for the preparation of quinoline-based hybrids i.e., (Z)-5-((Z)-benzylidene)-2-(quinolin-3-ylimino)thiazolidin-4-ones (QYT-4a-i) is outlined in Scheme 1 and the details are given in the Supplementary information.



Scheme 1: Synthesis of new target molecules (QYT-4a-i)

In the first step, 3-Aminoquinoline (**1**) was reacted with chloroacetyl chloride in dimethylformamide (DMF) at room temperature to synthesize 2-chloro-N-(quinolin-3-yl)acetamide (**2**), the compound **2** subsequently subjected to cyclization reaction in the presence of ammonium thiocyanate to produce the substituted 4-thiazolidinone (**3**) (Amin, Rahman, & Al-Eryani, 2008) in excellent yield (Supplementary table). Finally, the compound (**3**) was reacted with various aromatic aldehydes to yield target molecules (QYT-4a-i) (Zhou et al., 2008).

2.2 *In vitro* inhibition assay

Quinoline-based hybrids possessing different substituents were dissolved in 100% dimethyl sulfoxide (DMSO) and screened *in vitro* as inhibitors for the purified *LdMetAP1* and *HsMetAP1* (as control) in 96-well plates according to previous report (Bhat, Jagruthi, Srinivas, Arifuddin, & Qureshi, 2020). Enzymes (0.5 μ M) were incubated with inhibitor hits in the concentration range 0 to 200 μ M, and metal supplements Fe(II), Mn(II) or Co(II) in the assay buffer 50 mM Tris-HCl (pH 7.5) at 37 °C for 30 min. After incubation, the fluorogenic substrate L-methionine-4-methylcoumaryl-7-amide (Met-MCA) was added and the residual activity recorded with Infinite M200 Pro spectrofluorometer (TECAN, Switzerland). The percentage decrease in the activity of

inhibited samples as compared to uninhibited control aminopeptidase reactions was taken as percent inhibition and the IC₅₀ determined to rank the hits as per their potency. Time course kinetics was run to determine the mode of action. All data was plotted in GraphPad Prism (San Diego, USA).

2.3 MTT assay and ADME properties

To determine cell cytotoxicity, MTT (3-(4, 5-dimethylthiazol-2-yl)-2, 5-diphenyltetrazolium bromide) assay was used as reported previously (Bhat, Jagruthi, Srinivas, Arifuddin, & Qureshi, 2020). Mouse embryonic fibroblast cells were incubated in complete Dulbecco's modified Eagle medium (DMEM) carrying 0, 50, 100, 150 and 200 μ M concentrations of QYT-4h for 48 hrs in 96-well plates. Subsequently, MTT solution (5 mg/ml) was added to all wells and subjected to incubation for 4 hrs at 37°C. The formazan crystals were dissolved with DMSO and slight shaking at 37°C. Cell viability was determined spectrophotometrically by taking absorbance of each well at λ 570 nm. Furthermore, physicochemical properties and druglikeness of molecule QYT-4h was evaluated using the program SwissADME (Daina, Michielin, & Zoete, 2017).

2.4 SPR and Fluorescence spectroscopic measurements

Both *LdMetAP1* and *HsMetAP1* enzymes were covalently coupled to a CM-5 dextran chip (GE Healthcare) using amine coupling. Surface plasmon resonance binding assays were performed and analyzed as published in our previous report (Bhat, Jagruthi, Srinivas, Arifuddin, & Qureshi, 2020). Fluorescence spectroscopic measurements were performed with 1 μ M of *LdMetAP1* enzyme and 0-10 μ M of QYT-4h at 25°C. Stern-Volmer quenching constant (K_{SV}) and binding constant (K_b) were determined with Stern-Volmer and modified Stern-Volmer equations, respectively as reported previously (Alam, Abdelhameed, Rajpoot, & Khan, 2016).

2.5 Heat denaturation assay

The heat denaturation of *LdMetAP1* with hit molecule QYT-4h was performed as reported earlier (Bhat, Jagruthi, Srinivas, Arifuddin, & Qureshi, 2020). Precisely, 3 μ M of enzyme in 10 mM potassium phosphate buffer (pH 7.2) and approximately 3 μ M of QYT-4h were incubated for 30 min at ambient temperature, and subjected to thermal denaturation in a 0.2 cm quartz cuvette on JASCO-J1500 CD spectropolarimeter. Spectral changes were monitored at 218 nm due to the predominant presence of β -sheet secondary structure in *LdMetAP1* in the temperature range of 330-373 K. The spectral data gathered was normalized and the thermodynamic parameters determined as reported previously (Bhat & Qureshi, 2020).

2.6 Molecular docking

The modelled structure of *LdMetAP1* reported previously (Bhat, Jagruthi, Srinivas, Arifuddin, & Qureshi, 2020) was used for molecular docking of QYT-4h with the program AutoDock Vina (Trott & Olson, 2010). The structure of lead molecule QYT-4h was drawn in ChemDraw (<https://www.perkinelmer.com/product/chemdraw-professional-chemdrawpro>) and its geometry optimized as reported here (Bhat, Dey, & Qureshi, 2018). Autodock tools used to generate inbuilt files for molecular docking following Lamarckian genetic algorithm (Fuhrmann, Rurainski, Lenhof, & Neumann, 2010). Before defining the docking parameters water molecules and hydrogens were removed and polar hydrogens were added and the grid was setup around active site residues (DDHEE) of *LdMetAP1* with 0.25 Å spacing, and dimensions 40x41x40. For docking of QYT-4h into *HsMetAP1* (PDB ID: 2B3K), grid dimensions 40x42x38 around catalytic active site was used. The structural coordinates were visualised in PyMOL (<http://www.pymol.org>).

2.7 Molecular dynamics

Program Gromacs 4.6.3 (Van Der Spoel et al., 2005) and GROMOS 96 43a1 force field were used to execute molecular dynamics simulations for 30 ns of *LdMetAP1* bound QYT-4h complex. The complex was solvated and neutralized by adding chloride ions. This generated an electro-neutral system which was energy minimized by steepest descent method to reduce steric clashes and enact a stable system. Pressure and temperature factors of the complex were stabilized by two canonical equilibration runs before beginning data collection for 30 ns as reported earlier (Bhat, Jagruthi, Srinivas, Arifuddin, & Qureshi, 2020).

3. Results

3.1 Discovery of QYT-4h as a specific catalytic inhibitor against *LdMetAP1*

The quinoline core containing derivatives have been reported to be antileishmanial agents (Upadhyay et al., 2018) and inhibitory for leishmanial methionine aminopeptidase 1 (Bhat, Jagruthi, Srinivas, Arifuddin, & Qureshi, 2020). Therefore, we synthesized a library of quinoline-based hybrids with substitutions in the sulphur containing pentameric ring linked to bicyclic quinoline core through a trivalent nitrogen atom (Supplementary table) followed by characterization using ¹H-NMR, ¹³C-NMR, Mass and FT-IR.

All newly synthesized quinoline-based hybrids were tested *in vitro* at a concentration of 100 µM against both of the *LdMetAP1* and *HsMetAP1* enzymes, purified to homogeneity (Supplementary figure) as reported earlier (Bhat, Jagruthi, Srinivas, Arifuddin, & Qureshi, 2020). In initial

screening, we found QYT-4h to be the only promising compound with significant potency for purified *LdMetAP1* (Table 1). Therefore, QYT-4h was further tested for selectivity in aminopeptidase inhibition assay in the concentration range of 0 to 200 μM . QYT-4h exhibited high specificity to *LdMetAP1* and had nearly 20-fold lower potency against *HsMetAP1* (Fig. 1A). We next performed kinetic assays of *LdMetAP1* enzyme in the absence and presence of QYT-4h molecule. Kinetic assay in the presence of QYT-4h showed an increase in Michealis constant (K_m) and had a steady maximal velocity (V_{max}) when compared to untreated aminopeptidase kinetic reactions, demonstrating *LdMetAP1* to be inhibited through a competitive mode of inhibition by QYT-4h (Fig. 1B). Alternatively, a series of experiments conducted separately with increasing substrate concentrations suggested a steady rise in IC_{50} which further supports the competitive mode of action of QYT-4h (Fig. 1C).

Sulphur containing pentameric ring of quinoline-carbaldehyde was substituted with a double bond and then a single bond to which different ring containing substituent groups were added. However, no group except an indole substitution appeared to increase the potency. Intriguingly, every group added had a ring structure either a single ring or a double ring which was substituted with different chemical groups (Supplementary table). However, despite ring substitutions (4a-i) in every molecule, only QYT-4h which has an indole substitution was selective and highly potent against *LdMetAP1*.

Afterwards, we checked the toxicity of hit molecule QYT-4h with an MTT assay using mouse embryonic fibroblast cells and found this molecule exhibiting very low toxicity (Table 2). While checking whether QYT-4h adheres to the modified Lipinski's rule, we determined its physicochemical and druglikeness. LogP which describes the behaviour of a potential drug in body should not exceed a value of 5 according to the Lipinski's rule (Benet et al., 2016) as a value higher than 5 ($\text{LogP} > 5$) renders it highly lipophilic which may lead to low solubility and insufficient oral absorption. Alternatively, highly lipophilic molecules have a tendency to associate with hydrophobic targets than reach the desired targets in cells causing toxicity. Likewise, a highly negative LogP makes it more hydrophilic and therefore, unable to cross biological membranes for effective action. Importantly, QYT-4h was predicted to have a LogP of 2.86 which falls within the permissible limits, and demonstrated high pharmacokinetics. Furthermore, QYT-4h also showed acceptable water solubility as demonstrated by its predicted LogS value (Table 2).

3.2 QYT-4h is more potent against physiologically relevant Mn(II) and Fe(II) forms of *LdMetAP1*

Methionine aminopeptidases (MetAPs) are mostly regarded as Fe(II) (Chai, Wang, & Ye, 2008) or Mn(II) (Wang et al., 2003) dependent aminopeptidases *in vivo*. A recent report on the metal dependence of leishmanial MetAP1 suggests its high catalytic efficiency with both Fe(II) and Mn(II), in particular with Fe(II), than Co(II) (Bhat, Jagruthi, Srinivas, Arifuddin, & Qureshi, 2020). Therefore, discovery or development of any new inhibitor against *LdMetAP1* should consider the inhibitor potency against the physiologically relevant Fe(II) and Mn(II) activated forms of this enzyme. Hence, IC₅₀ of newly identified *LdMetAP1* inhibitor QYT-4h was determined with both physiologically relevant Fe(II) and Mn(II) along with Co(II) supplemented forms of this enzyme. Intriguingly, inhibitor potency (IC₅₀) of QYT-4h was best when *LdMetAP1* was supplemented with either Mn(II) or Fe(II) than the Co(II) supplemented form (Fig. 1D-I) rendering QYT-4h most effective against the physiologically relevant Mn(II) and Fe(II) forms of *LdMetAP1*.

3.3 QYT-4h binds to *LdMetAP1* with high affinity

Using SPR binding assays, we tracked the physical interactions of *LdMetAP1* and *HsMetAP1* enzymes with QYT-4h inhibitor. SPR sensorgrams demonstrated a direct interaction between QYT-4h and recombinant enzymes with elevated affinity to both *LdMetAP1* and *HsMetAP1*. The lead inhibitor molecule QYT-4h bound both enzymes with higher affinity and exhibited slower off-rate, yet QYT-4h has remarkably higher inhibitor potency against *LdMetAP1* (Fig. 2A-B). As an additional affirmation that QYT-4h had high affinity for *LdMetAP1*, we employed fluorescence spectroscopy which demonstrated a concentration dependent (0 to 10 μM) fluorescence quenching of *LdMetAP1* indicating a complex formation, and determined the quenching constant and binding constant of QYT-4h for both enzymes. A very high association constant of QYT-4h was observed for both enzymes (Fig. 2C-H) which matches with the results deduced from SPR binding assays.

3.4 Structural basis of inhibition of *LdMetAP1* by QYT-4h

Molecular docking was performed to definitively unravel the binding mode and atomic interactions of QYT-4h with *LdMetAP1* and its human counterpart *HsMetAP1*. Thus, the conformation of lead molecule QYT-4h with greatest binding affinity with receptors *LdMetAP1*

and *HsMetAP1* was selected for determining the binding site and the atomic interactions involved. In *LdMetAP1* structure (Bhat, Jagruthi, Srinivas, Arifuddin, & Qureshi, 2020), QYT-4h bound at the catalytic active site as also demonstrated by biochemistry guided assays (Fig. 1B and C). QYT-4h interacted with *LdMetAP1* through a strong bifurcated salt bridge involving residues Thr291 and Gly292, and a hydrogen bond through nitrogen atom of sulphur containing pentameric ring with Thr291 (Fig. 3A). Additionally, QYT-4h had hydrophobic interactions with residues Arg107, Tyr185, Tyr186, His300, Thr301, Ala302 and Asn304. Interestingly, the binding of QYT-4h with *LdMetAP1* match considerably with those of HQ14 and HQ15 inhibitor molecules with this enzyme (Bhat, Jagruthi, Srinivas, Arifuddin, & Qureshi, 2020). A major highlight of the binding mode of QYT-4h was its ability to occupy the catalytic site along with S1 and S1' sub-sites of *LdMetAP1*. However, QYT-4h binds to *HsMetAP1* (PDB ID: 2B3K) with a different binding mode involving a salt bridge with Tyr196 and hydrogen bonds with Tyr195 and Thr311, and hydrophobic interactions with residues Glu128, Gln129, Leu131, Lys132, Gly133, Thr134, Tyr196, Tyr300, His310 and Ala312 (Fig. 3B). Inability of QYT-4h to protrude into the smaller catalytic pocket of *HsMetAP1* provides structural basis for the significant potency of QYT-4h against *LdMetAP1* but not *HsMetAP1*.

3.5 Complex of *LdMetAP1* with QYT-4h exhibits stability and compactness

The QYT-4h bound *LdMetAP1* complex was simulated for 30 ns and the stability of the complex was analysed with group parameters including root mean square deviation (RMSD), root mean square fluctuation (RMSF) and radius of gyration (Rg). To compare, the data of unliganded *LdMetAP1* (Bhat, Jagruthi, Srinivas, Arifuddin, & Qureshi, 2020) structure was used to study the differences in RMSD after ligand binding. It is apparent that QYT-4h binding caused some perturbations in the RMSD of *LdMetAP1* (Fig. 4A). This possibly meant some changes or adjustments in the *LdMetAP1* secondary structure after QYT-4h binding. However, it is evident that QYT-4h binding didn't induce any major changes in structure as *LdMetAP1*-QYT-4h complex reached to equilibrium and formed a stable complex.

Alternatively, we analysed flexibility and compactness by parameters RMSF and Rg. Residues holding QYT-4h in the catalytic pocket of *LdMetAP1* with hydrogen bonding and hydrophobic interactions showed a steady RMSF suggesting the complex of QYT-4h with *LdMetAP1* to be rigid during the course of production run (Fig. 4B). However, fluctuations occurred in a specific C-terminal region precisely in a group of residues which didn't appear to have a role in QYT-4h

binding. It was interesting to find that the non-catalytic residues Cys221 and Ser250 which have been reported to be highly flexible in apo *LdMetAP1* (Bhat, Jagruthi, Srinivas, Arifuddin, & Qureshi, 2020) showed steadiness in *LdMetAP1*-QYT-4h complex. The complex also showed high degree of compactness (Fig. 4C). This suggests complex formation with QYT-4h stabilizes *LdMetAP1*. The 30 ns production run highlighted slight changes in RMSD and secondary structure after QYT-4h binding, which indicate conformational rearrangements occurring in *LdMetAP1*.

Such a pattern in RMSD and structure of *LdMetAP1* has also been reported with another quinoline core bearing inhibitor molecule HQ15 of our recently published work (Bhat, Jagruthi, Srinivas, Arifuddin, & Qureshi, 2020). As the thermal stability parameters of *LdMetAP1* are known (Bhat, Jagruthi, Srinivas, Arifuddin, & Qureshi, 2020), we employed a heat denaturation assay which demonstrated that QYT-4h formed a very stable complex with *LdMetAP1* as thermo-stability of complex drifted right (Fig. 4D). Therefore, SPR binding assays, spectroscopic methods and molecular dynamics demonstrate high affinity and a very stable complex formation between hit molecule QYT-4h and *LdMetAP1*.

4. Discussion

N-terminal methionine processing is a vital and evolutionary conserved process occurring in both lower and higher organisms. Eukaryotes including humans, yeast and *Leishmania* species express both MetAP1 and MetAP2 whose deletion leads to the development of lethal phenotypes (Li & Chang, 2006). Additionally, inhibition or inactivation of MetAPs with specific small molecule agents causes immune suppression (Priest et al., 2009), impedes angiogenesis (Sin et al., 2002) and leads to parasitic death (Chen et al., 2006). A recent report suggests the druggability of leishmanial MetAP1 (*LdMetAP1*) and the ability of small molecule inhibitors to cause the death of leishmanial parasite both *in vitro* and *in vivo* (Rodriguez et al., 2020). Therefore, given the essentiality and potential druggability of MetAPs, we have tested quinoline-based hybrids i.e., [(Z)-5-((Z)-benzylidene)-2-(quinolin-3-ylimino)thiazolidin-4-ones] (QYT-4a-i) as novel inhibitors and discovered QYT-4h which carries an indole substitution as a new and specific inhibitor of leishmanial MetAP1. Importantly, QYT-4h demonstrated an approximate 20-fold lower potency against human methionine aminopeptidase 1 (*HsMetAP1*). Another important feature of QYT-4h was its significant potency for Fe(II) supplemented *LdMetAP1* which assumes significance as methionine aminopeptidases (MetAPs) are usually categorized as Mn(II) (Wang et al., 2003) or

Fe(II) (D'souza & Holz, 1999; Chai, Wang, & Ye, 2008) dependent aminopeptidases *in vivo* than Co(II) dependent aminopeptidases. As MetAP enzymes demonstrate high catalytic activity with divalent metals and usually exhibit specificity to a certain metal co-factor, designing inhibitors with high metal sequestration property might play a front-runner role towards new inhibitor discovery or drug development. We have previously shown *LdMetAP1* to exhibit high catalytic efficiency with Fe(II) (Bhat, Jagruthi, Srinivas, Arifuddin, & Qureshi, 2020). This possibly happens because metal-ligand interactions may be very specific which enables *LdMetAP1* to show high specificity for substrates when activated with Fe(II). Meanwhile, most metal requiring enzymes in general and aminopeptidases in particular are activated by many metal ions. This is because the binding of metal ions to aminopeptidase is also electrostatic allowing several different metal ions with identical sizes and charges to act as co-factors, and cause enzyme activation. Any promising inhibitor of metal-dependent aminopeptidases found through high throughput screening or random screening of inhibitor libraries carrying heteroatoms in a hydrophobic environment such as QYT-4h may offer a framework for involvement in complex formation with active site metal ions leading to enzyme inhibition through a non-covalent mode (Mucha et al., 2010). Thus, potency of newly discovered inhibitors against different forms of metal activated enzyme becomes inevitable. However, high potency of an inhibitor against a biologically relevant metal activated form of enzyme attains significance. Pertinently, small molecules inhibitors targeting MetAP1 eliminate leishmanial parasites and have a potential to develop into new frontline antileishmanial agents (Rodriguez et al., 2020).

Realizing that any newly discovered inhibitor should not only demonstrate potency or specificity but high binding association or affinity for the target enzyme, we employed surface plasmon resonance and spectroscopic methods which also demonstrated high affinity of QYT-4h molecule for *LdMetAP1* along with a stable complex formation. This was largely in line with molecular dynamics which showed that the complex between *LdMetAP1* and QYT-4h was rigid and exhibited greater compactness and lesser flexibility. A notable and significant feature of QYT-4h was its promising potency for leishmanial MetAP1 enzyme and not its human counterpart. The structural and molecular basis for the substantial differences in potency of QYT-4h towards orthologous MetAPs is still incomprehensible, however, specificity may be due to differences in amino acids composition of *LdMetAP1* and *HsMetAP1* within the 6 Å distance from the catalytic site as also reported previously (Bhat, Jagruthi, Srinivas, Arifuddin, & Qureshi, 2020). Bulkier amino acid residues near the catalytic active site of *HsMetAP1* render its metal dependent catalytic

site highly compact, thus less accessible to quinoline core containing QYT-4h and less susceptible to inhibition.

5. Conclusions

In this study, we report the discovery of a novel and specific quinolone-based hybrid (QYT-4h) inhibitor against the methionine aminopeptidase 1 of *L. donovani* (*LdMetAP1*). This molecule was twenty-fold less specific to the recombinant human MetAP1 and exhibited drug-like properties. Remarkably, QYT-4h demonstrated high association and affinity with *LdMetAP1* and formed a highly stable complex with this enzyme. Other important attributes associated with QYT-4h were its competitive mode of action, and significant potency against the physiologically relevant Fe(II) and Mn(II) forms of *LdMetAP1*. Small molecule inhibitors specific to *LdMetAP1* have a potential to bypass the havoc caused by spread of leishmanial parasites and the drug resistance linked to some parasitic forms which has in turn blockaded the effective annulment of leishmaniasis. Thus, the discovery of drug-like molecules like QYT-4h definitively targeting *LdMetAP1* can aid in the development of new chemotherapeutic molecules. Moreover, specific inhibition of *LdMetAP1* offers an advantage to stop the growth and proliferation of both life forms (promastigotes and amastigotes) of *L. donovani* as *LdMetAP1* is a house-keeping protein. This extends the importance of newly discovered *LdMetAP1* inhibitors, such as QYT-4h, which provides an inhibitor scaffold whose improvement in selectivity and potency towards *LdMetAP1* but not *HsMetAP1* can guide the development of novel, selective and potent antileishmanial agents.

Acknowledgements

This work was financially supported by a grant from Council of Scientific and Industrial Research (CSIR, project no. 37(1686)/17/EMR-II) to IAQ. SYB thanks Indian Council of Medical Research (ICMR) for Senior Research Fellowship. SB, PST and MA are grateful to Department of Pharmaceuticals, Ministry of Chemicals and Fertilizers, Government of India for financial support in the form of M.S. and Ph.D. scholarships. The authors also acknowledge the instruments facilities supported by DST-FIST and UGC-SAP to Department of Biotechnology & Bioinformatics, and Bioinformatics Infrastructure Facility, School of Life Sciences for computational resources. The authors declare that they have no competing interests.

Data Availability Statement

The data that supports the findings of this study are available in the supplementary material of this article.

References

- Addlagatta, A., Hu, X., Liu, J. O. & Matthews, B. W. (2005). Structural basis for the functional differences between type I and type II human methionine aminopeptidases. *Biochemistry*, **44**, 14741-14749. <https://doi.org/10.1021/bi051691k>
- Alam, P., Abdelhameed, A. S., Rajpoot, R. K., & Khan, R. H. (2016). Interplay of multiple interaction forces: Binding of tyrosine kinase inhibitor nintedanib with human serum albumin. *Journal of Photochemistry and Photobiology B: Biology*, **157**, 70-76. <https://doi.org/10.1016/j.jphotobiol.2016.02.009>
- Alvar, J., Vélez, I. D., Bern, C., Herrero, M., Desjeux, P., Cano, J., Jannin, J., & de Boer, M. (2012). Leishmaniasis worldwide and global estimates of its incidence. *PLoS ONE*, **7**, e35671. <https://doi.org/10.1371/journal.pone.0035671>
- Amin, K. M., Rahman, D. E. A., & Al-Eryani, Y. A. (2008). Synthesis and preliminary evaluation of some substituted coumarins as anticonvulsant agents. *Bioorganic and Medicinal Chemistry*, **16**, 5377-88. <https://doi.org/10.1016/j.bmc.2008.04.021>
- Bernier, S. G., Lazarus, D. D., Clark, E., Doyle, B., Labenski, M. T., Thompson, C. D., Westlin, W. F., & Hannig, G. (2004). A methionine aminopeptidase-2 inhibitor, PPI-2458, for the treatment

of rheumatoid arthritis. *Proceedings of the National Academy of Sciences of the United States of America*, **101**, 10768-10773. <https://doi.org/10.1073/pnas.0404105101>

Bhat, S. Y., & Qureshi, I. A. (2020). Mutations of key substrate binding residues of leishmanial peptidase T alter its functional and structural dynamics. *Biochimica et Biophysica Acta- General Subjects*, **1864**, 129465. <https://doi.org/10.1016/j.bbagen.2019.129465>

Bhat, S. Y., Dey, A., & Qureshi, I. A. (2018). Structural and functional highlights of methionine aminopeptidase 2 from *Leishmania donovani*. *International Journal of Biological Macromolecules* **115**, 940-954. <https://doi.org/10.1016/j.ijbiomac.2018.04.090>

Bhat, S.Y., Jagruthi, P., Srinivas, A., Arifuddin, M., & Qureshi, I. A. (2020). Synthesis and characterization of quinoline-carbaldehyde derivatives as novel inhibitors for leishmanial methionine aminopeptidase 1. *European Journal of Medicinal Chemistry*, **186**, 111860. <https://doi.org/10.1016/j.ejmech.2019.111860>

Benet, L. Z., Hosey, C. M., Ursu, O., & Oprea, T. I. (2016). BDDCS, the Rule of 5 and drugability. *Advanced Drug Delivery Reviews*, **101**, 89-98. <https://doi.org/10.1016/j.addr.2016.05.007>

Mucha, A., Drag, M., Dalton, J. P., & Kafarski, P. (2010). Metallo-aminopeptidase inhibitors. *Biochimie*, **92**, 1509-1529. <https://doi.org/10.1016/j.biochi.2010.04.026>

Bradshaw, R.A. (2013). Aminopeptidases. In: W.J. Lennarz and M.D. Lane (Eds.), *Encyclopedia of Biological Chemistry* (2nd Edition). Academic Press, pp. 97-99.

Burza, S., Croft S. L., & Boelaert, M. (2018). Leishmaniasis. *The Lancet*, **392**, 951-970. [https://doi.org/10.1016/S0140-6736\(18\)31204-2](https://doi.org/10.1016/S0140-6736(18)31204-2)

Chai, S. C., Wang, W. L., & Ye, Q. Z. (2008). Fe(II) is the native cofactor for *Escherichia coli* methionine aminopeptidase. *Journal of Biological Chemistry*, **283**, 26879-26885. <https://doi.org/10.1074/jbc.M804345200>

Chang, S. Y., McGary, E. C., & Chang, S. (1989). Methionine aminopeptidase gene of *Escherichia coli* is essential for cell growth, *Journal of Bacteriology*, **171**, 4071-4072. <https://doi.org/10.1128/jb.171.7.4071-4072.1989>

Chen, X., Chong, C. R., Shi, L., Yoshimoto, T., Sullivan, D. J., & Liu, J. O. (2006). Inhibitors of *Plasmodium falciparum* methionine aminopeptidase 1b possess antimalarial activity. *Proceedings*

of the National Academy of Sciences of the United States of America, **103** 14548-14553.
<https://doi.org/10.1073/pnas.0604101103>

D'souza, V. M., & Holz, R. C. (1999). The methionyl aminopeptidase from *Escherichia coli* can function as an iron(II) enzyme? *Biochemistry*, **38**, 11079-11085.
<https://doi.org/10.1021/bi990872h>

Daina, A., Michielin, O., & Zoete, V. (2017). SwissADME: A free web tool to evaluate pharmacokinetics, drug-Likeness and medicinal chemistry friendliness of small molecules. *Scientific Reports*, **7**, 42717. <https://doi.org/10.1038/srep42717>

Frottin, F., Bienvenut, W. V., Bignon, J., Jacquet, E., Sebastian, Vaca Jacome, A., Van Dorsselaer, A., Cianferani, S., Carapito, C., Meinel, T., & Giglione, C. (2016). MetAP1 and MetAP2 drive cell selectivity for a potent anti-cancer agent in synergy, by controlling glutathione redox state. *Oncotarget*, **7**, 63306-63323. <https://doi.org/10.18632/oncotarget.11216>

Fuhrmann, J., Rurainski, A., Lenhof, H. P., & Neumann, D. (2010). A new Lamarckian genetic algorithm for flexible ligand-receptor docking. *Journal of Computational Chemistry*, **31**, 1911-1918. <https://doi.org/10.1002/jcc.21478>

Giglione C., Boularot A., & Meinel T. (2004). Protein N-terminal methionine excision. *Cellular and Molecular Life Sciences*, **61**, 1455-1474. <https://doi.org/10.1007/s00018-004-3466-8>

Li, X., & Chang, Y. H. (2006). Amino-terminal protein processing in *Saccharomyces cerevisiae* is an essential function that requires two distinct methionine aminopeptidases. *Proceedings of the National Academy of Sciences of the United States of America*, **92**, 12357-12361. <https://doi.org/10.1073/pnas.92.26.12357>

Mohapatra, S. (2014). Drug resistance in leishmaniasis: Newer developments. *Tropical Parasitology*, **4**, 4-9. <https://doi.org/10.4103/2229-5070.129142>

Priest, R. C., Spaul, J., Buckton, J., Grimley, R. L., Sims, M., Binks, M., & Malhotra, R. (2009). Immunomodulatory activity of a methionine aminopeptidase-2 inhibitor on B cell differentiation. *Clinical and Experimental Immunology*, **155**, 514-522. <https://doi.org/10.1111/j.1365-2249.2008.03843.x>

Sin, N., Meng, L., Wang, M. Q. W., Wen, J. J., Bornmann, W. G., & Crews, C. M. (2002). The anti-angiogenic agent fumagillin covalently binds and inhibits the methionine aminopeptidase,

MetAP-2. *Proceedings of the National Academy of Sciences of the United States of America*, **94**, 6099-6103. <https://doi.org/10.1073/pnas.94.12.6099>

Rodriguez, F., John, S. F., Iniguez, E., Montalvo, S., Michael, K., White, L., Liang, D., Olaleye, O. A., & Maldonado, R. A. (2020). *In vitro* and *in vivo* characterization of potent antileishmanial methionine aminopeptidase 1 inhibitors. *Antimicrobial Agents and Chemotherapy*, **64**, e01422-19. <https://doi.org/10.1128/AAC.01422-19>

Sundar, S., & Chakravarty, J. (2010). Antimony toxicity. *International Journal of Environmental Research and Public Health*, **7**, 4267-4277. <https://doi.org/10.3390/ijerph7124267>

Thakur, L., Singh, K. K., Shanker, V., Negi, A., Jain, A., Matlashewski, G., & Jain, M. (2018). Atypical leishmaniasis: A global perspective with emphasis on the Indian subcontinent. *PLoS Neglected Tropical Diseases*, **12**, e0006659. <https://doi.org/10.1371/journal.pntd.0006659>

Trott, O., & Olson, A. J. (2010). AutoDock Vina: improving the speed and accuracy of docking with a new scoring function, efficient optimization and multithreading. *Journal Computational Chemistry*, **31**, 445- 461. <https://doi.org/10.1002/jcc.21334>

Upadhyay, A., Kushwaha, P., Gupta, S., Dodda, R. P., Ramalingam, K., Kant, R., Goyal, N., & Sashidhara, K. V. (2018). Synthesis and evaluation of novel triazolyl quinoline derivatives as potential antileishmanial agents. *European Journal of Medicinal Chemistry*, **154**, 172- 181. <https://doi.org/10.1016/j.ejmech.2018.05.014>

Van Der Spoel, D., Lindahl, E., Hess, B., Groenhof, G., Mark, A. E., & Berendsen, H. J. C. (2005). GROMACS: Fast, flexible, and free. *Journal of Computational Chemistry*, **26**, 1701-1718. <https://doi.org/10.1002/jcc.20291>

Wang, J., Sheppard, G. S., Lou, P., Kawai, M., Park, C., Egan, D. A., Schneider, A., Bouska, J., Lesniewski, R., & Henkin, J. (2003). Physiologically relevant metal cofactor for methionine aminopeptidase-2 is manganese. *Biochemistry*, **42**, 5035- 5042. <https://doi.org/10.1021/bi020670c>

Yin, S. Q., Wang, J. J., Zhang, C. M., & Liu, Z. P. (2012). The development of MetAP-2 inhibitors in cancer treatment. *Current Medicinal Chemistry*, **19**, 1021- 1035. <https://doi.org/10.2174/092986712799320709>

Zhang, P., Nicholson, D. E., Bujnicki, J. M., Su, X., Brendle, J. J., Ferdig, M., Kyle, D. E., Milhous, W. K., & Chiang, P. K. (2002). Angiogenesis inhibitors specific for methionine

aminopeptidase 2 as drugs for malaria and leishmaniasis. *Journal of Biomedical Science*, **9**, 34-40. <https://doi.org/10.1007/BF02256576>

Zhou, H., Wu, S., Zhai, S., Liu, A., Sun, Y., Li, R., Zhang, Y., Ekins, S., Swaan, P. W., Fang, B., Zhang, B., & Yan, B. (2008). Design, synthesis, cytoselective toxicity, structure-activity relationships, and pharmacophore of thiazolidinone derivatives targeting drug-resistant lung cancer cells. *Journal of Medicinal Chemistry*, **51**, 1242- 1251. <https://doi.org/10.1021/jm7012024>

Zijlstra, E. E. (2016). The immunology of post-kala-azar dermal leishmaniasis (PKDL). *Parasites and Vectors*, **9**, 464. <https://doi.org/10.1186/s13071-016-1721-0>

Tables:

Table 1. IC₅₀ values of quinoline-based hybrids (QYT-4a-i) against purified *LdMetAP1* and *HsMetAP1* determined by variable slope method. Data is given as mean ± S.D. of three experiments.

Compound	<i>LdMetAP1</i> IC ₅₀ (μM)	<i>HsMetAP1</i> IC ₅₀ (μM)
QYT-4a	52.2 ± 3.7	>200
QYT-4b	59.0 ± 3.2	156.5 ± 17.6
QYT-4c	116.3 ± 11.4	>200
QYT-4d	89.1 ± 6.5	>200
QYT-4e	67.1 ± 6.3	Very far
QYT-4f	123.4 ± 11.5	>200
QYT-4g	66.4 ± 5.6	>200
QYT-4h	3.0 ± 0.4	58.0 ± 4.4
QYT-4i	27.4 ± 3.2	54.2 ± 6.5

Table 2. ADME properties of QYT-4h and cell viability analysis

Compound	Molecular Weight (g/mol)	LogP	LogS	Pharmacokinetics	Drug likeness	Cytotoxicity (μM)
QYT-4h	370.42	2.86	-4.59	High	Yes	>150

Figures:

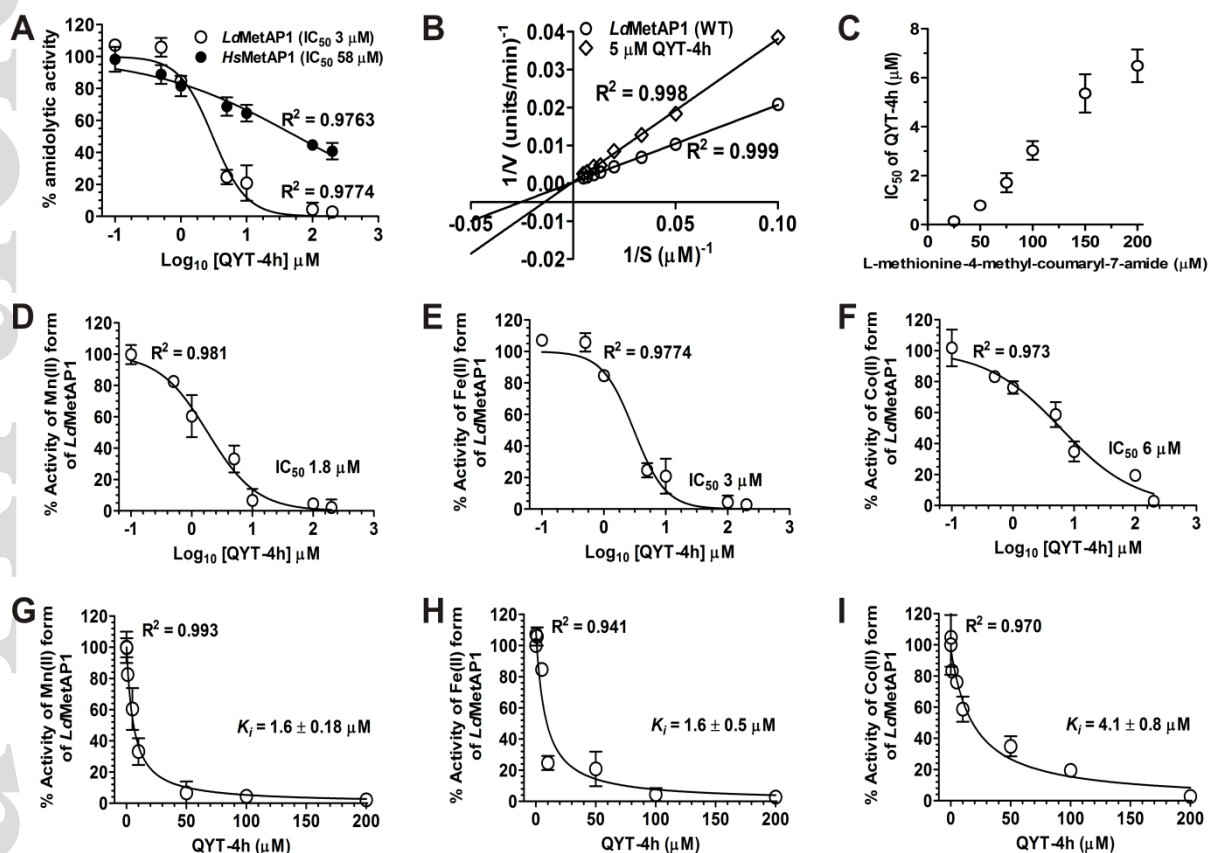


Figure 1: Aminopeptidase inhibition showing metal dependence. (A) Inhibition of aminopeptidase activity of *LdMetAP1* and *HsMetAP1* with QYT-4h. (B) Lineweaver-Burk plot demonstrating the competitive mode of inhibition of *LdMetAP1* with QYT-4h inhibitor. (C) QYT-4h is a competitive catalytic binding site inhibitor of *LdMetAP1*. IC_{50} values were determined as depicted in fig. 1A. (D and G) Inhibition of Mn(II) form of *LdMetAP1* with QYT-4h. (E and H) Inhibition of Fe(II) form of *LdMetAP1* with QYT-4h. (F and I) Inhibition of Co(II) form of *LdMetAP1* with QYT-4h. Error bars represent mean \pm SD of three experiments performed in triplicates.

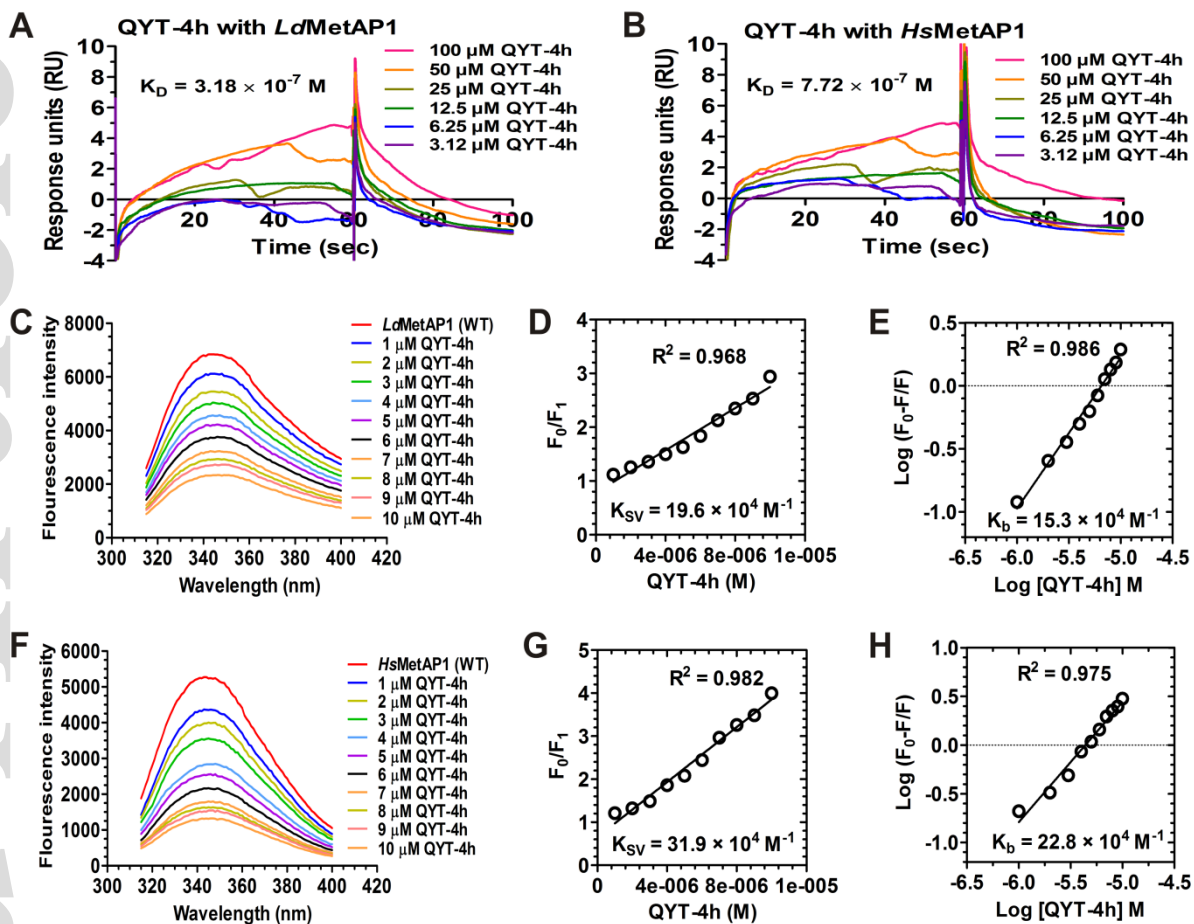


Figure 2: QYT-4h has high affinity for *LdMetAP1*. SPR sensorgrams (A and B) showing the binding of QYT-4h with recombinant *LdMetAP1* and *HsMetAP1* immobilized on CM-5 sensor chip. Data shown is a mean of two independent experiments performed at ambient temperature. Fluorescence spectra (C and F), Stern-Volmer plots (D & G) and modified Stern-Volmer plots (E & H) of recombinant *LdMetAP1* and *HsMetAP1* with QYT-4h compound.

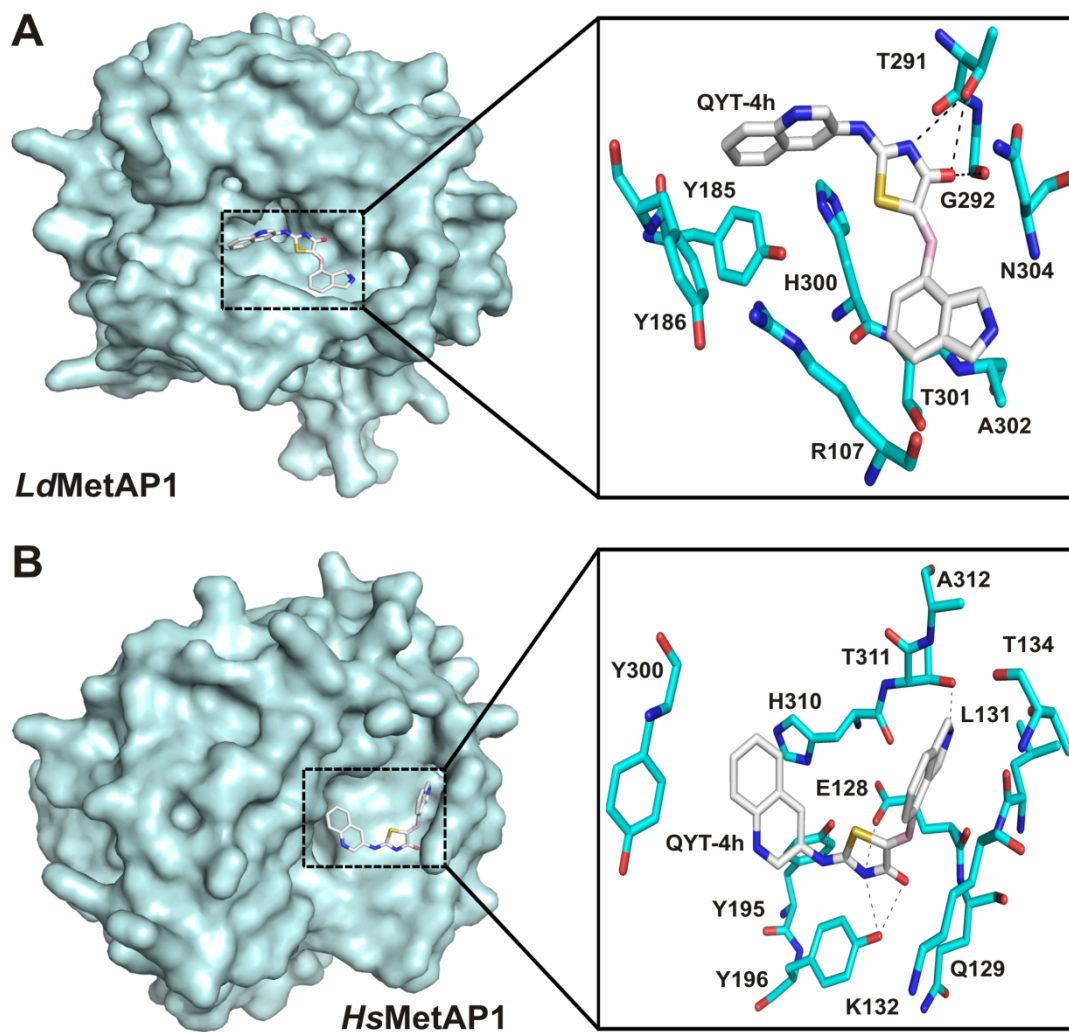


Figure 3: Molecular docking of QYT-4h with modelled *LdMetAP1* and crystal structure of *HsMetAP1* (PDB ID: 2B3K). Structures of *LdMetAP1* and *HsMetAP1* (as surface) docked with QYT-4h (shown as sticks) are shown with enlarged view of the atomic interactions of QYT-4h with *LdMetAP1* and *HsMetAP1*. Black dashed lines demonstrate salt bridges and hydrogen bonding, whereas interacting residues are represented as sticks.

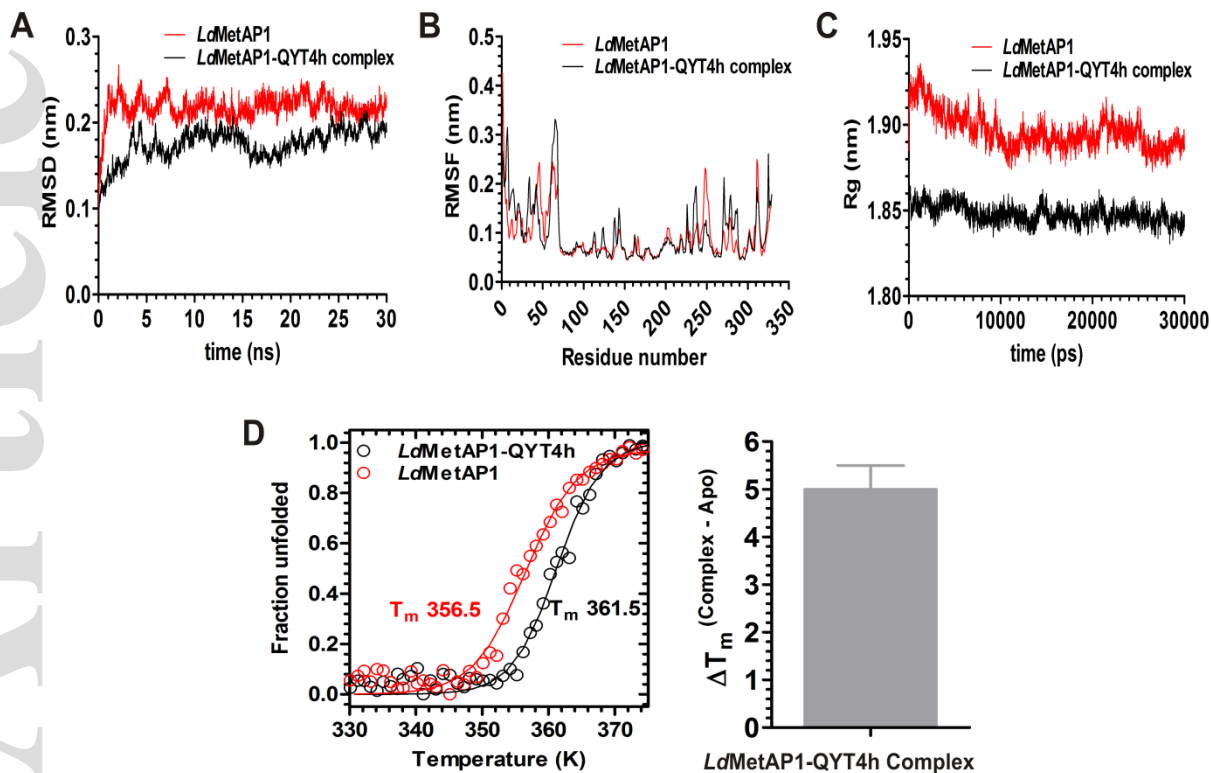


Figure 4: Molecular dynamics. (A) RMSD of *LdMetAP1* and its complex with QYT-4h. (B) RMSF of *LdMetAP1* and its complex with QYT-4h for 30 ns production run. (C) Radius of gyration of enzyme *LdMetAP1* without and in complex with QYT-4h. (D) Heat denaturation plot highlighting an increase in the thermo-stability of *LdMetAP1* after its complex formation with QYT-4h. Error bar represents mean \pm SD of two scans.